Annex A: Examples on estimation of uncertainty in airflow measurement

Introduction

This annex contains three examples of fluid flow measurement uncertainty analysis. The first deals with airflow measurement for an entire facility (with several test stands) over a long period. It also applies to a single test with a single set of instruments. The second example demonstrates how comparative development tests can reduce the uncertainty of the first example. The third example illustrates a liquid flow measurement.

A.1 General

Airflow measurements in gas turbine engine systems are generally made with one of three types of flowmeters: venturis, nozzles and orifices. Selection of the specific type of flowmeter to use for a given application is contingent upon a tradeoff between measurement accuracy requirements, allowable pressure drop and fabrication complexity and cost.

Flowmeters may be further classified into two categories: subsonic flow and critical flow. With a critical flowmeter, in which sonic velocity is maintained at the flowmeter throat, mass flowrate is a function only of the upstream gas properties. With a subsonic flowmeter, where the throat Mach number is less than sonic, mass flowrate is a function of both upstream and downstream gas properties.

Equations for the ideal mass flowrate through nozzles, venturies and orifices are derived from the continuity equation:

$$W = \rho a V \qquad (39)$$

In using the continuity equation as a basis for ideal flow equation derivations, it is normal practice to assume conservation of mass and energy and one-dimensional isentropic flow. Expressions for ideal flow will not yield actual flow since actual conditions always deviate from ideal. An empirically determined correction factor, the discharge coefficient (C) is used to adjust ideal to actual flow:

$$C = W_{actual}/W_{ideal} \qquad (40)$$

A.2 Example one — test facility

A.2.1 Definition of the measurement process

What is the airflow measurement capability of a given industrial or government test facility? This question might relate to a guarantee in a product specification or a research contract. Note that this question implies that many test stands, sets of instrumentation and calibrations over a long period of time should be considered.

The same general uncertainty model is applied in the second example to a single stand process, the comparative test.

These examples will provide, step by step, the entire process of calculating the uncertainty of the airflow parameter. The first step is to understand the defined measurement process and then identify the source of every possible error. For each measurement, calibration errors will be discussed first, then data acquisition errors, data reduction errors, and finally, propagation of these errors to the calculated parameter.

Figure 14 depicts a critical venturi flowmeter installed in the inlet ducting upstream of a turbine engine under test for this example.

When a venturi flowmeter is operated at critical pressure ratios, i.e., (P_2/P_1) is a minimum, the flowrate through the venturi is a function of the upstream conditions only and may be calculated from

$$W = \frac{\pi d^2}{4} C F_a \varphi^* \frac{P_1}{\sqrt{T_1}} \qquad (41)$$

A.2.2 Measurement error sources

Each of the variables in equation 41 must be carefully considered to determine how and to what extent errors in the determination of the variable affect the calculated parameter. A relatively large error in some will affect the final answer very little, whereas small errors in others have a large effect. Particular care should be taken to identify measurements that influence the fluid flow parameters in more than one way.

In equation (41), upstream pressure and temperature (P_1 and T_1) are of primary concern. Error sources for each of these measurements are: (1) calibration, (2) data acquisition and (3) data reduction.

A.2.2.1 Figure 15 illustrates a typical calibration hierarchy. Associated with each comparison in the calibration hierarchy is a possible pair of elemental errors, a systematic error limit and an experimental standard deviation. Table 7 lists all of the elemental errors. Note that these elemental errors are not cumulative, e.g., B_{21} is not a function of B_{11}. The systematic error limits should be based on interlaboratory tests if available, otherwise, the judgment of the best experts must be used. The experimental standard deviations are calculated from calibration history data banks.

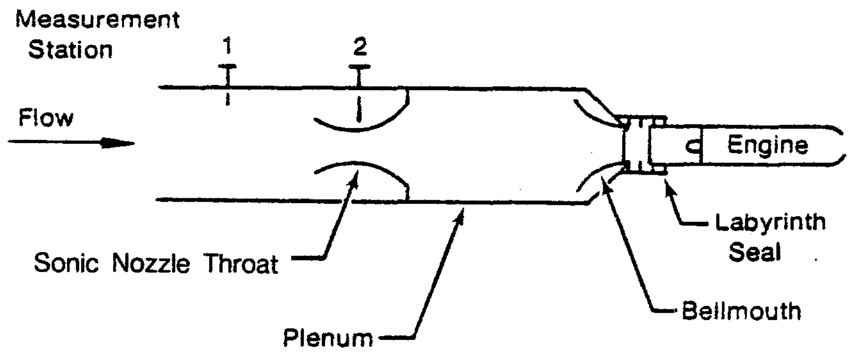

Figure 14 — Schematic of sonic nozzle flowmeter installation upstream of a turbine engine

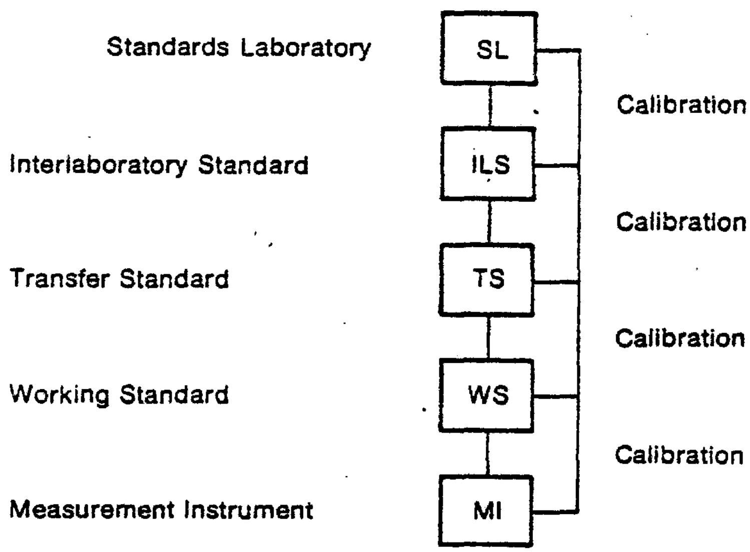

Figure 15 — Typical calibration hierarchy

Table 7 — Calibration hierarchy error sources

Calibration	*Systematic error, P_a*	*Experimental standard deviation, P_a*	*Degrees of freedom*
SL - ILS	B_{11} = 68.953	S_{11} = 13.787	ν_{11} = 10
ILS-TS	B_{21} = 68.953	S_{21} = 13.787	ν_{21} = 15
TS - WS	B_{31} = 68.953	S_{31} = 13.787	ν_{31} = 20
WS - MI	B_{41} = 124.	S_{41} = 36.541	ν_{41} = 30

The experimental standard deviation for the calibration process is the root-sum-square of the elemental sample standard deviations, i.e.,

$$S_1 = \sqrt{S_{11}^2 + S_{21}^2 + S_{31}^2 + S_{41}^2}$$

$$= \sqrt{13.787^2 + 13.787^2 + 13.787^2 + 36.541^2}$$

$$= 43.65 \text{ P}_a \tag{42}$$

Degrees of freedom associated with S are calculated from the Welch-Satterthwaite formula as follows:

$$\nu_1 = \frac{(S_{11}^2 + S_{21}^2 + S_{31}^2 + S_{41}^2)^2}{\left(\frac{S_{11}^4}{\nu_{11}} + \frac{S_{21}^4}{\nu_{21}} + \frac{S_{31}^4}{\nu_{31}} + \frac{S_{41}^4}{\nu_{41}}\right)}$$

$$= \frac{(13.787^2 + 13.787^2 + 13.787^2 + 36.541^2)^2}{\left(\frac{13.787^4}{10} + \frac{13.787^4}{15} + \frac{13.787^4}{20} + \frac{36.541^4}{30}\right)} = 54. \tag{43}$$

The systematic error for the calibration process is the root-sum-square of the elemental systematic error limits, i.e.,

$$B_1 = \sqrt{B_{11}^2 + B_{21}^2 + B_{31}^2 + B_{41}^2} \tag{44}$$

$$= \sqrt{68.953^2 + 68.953^2 + 68.953^2 + 124.117^2}$$

$$= 172.2 \text{ P}_a \tag{45}$$

Data acquisition error sources for pressure measurement are listed in table 8.

Table 8 — Pressure transducer data acquisition error sources

Error source	*Systematic error, P_a*	*Experimental standard Deviation, P_a*	*Degrees of freedom*
Excitation Voltage	B_{12} = 68.953	S_{12}= 34.481	ν_{12} = 40
Electrical Simulation	B_{22} = 68.953	S_{22} = 34.481	ν_{22} = 90
Signal Conditioning	B_{32} = 68.953	S_{32} = 34.481	ν_{32} = 200
Recording Device	B_{42} = 68.953	S_{42} = 34.481	ν_{42} = 10
Pressure Transducer	B_{52} = 68.953	S_{52} = 48.270	ν_{52} = 100
Environmental Effects	B_{62} = 68.953	S_{62} = 68.953	ν_{62} = 10
Probe Errors	B_{72} = 117.223	S_{72} = 48.270	ν_{72} = 60

The experimental standard deviation for the data acquisition process is

$$S_2 = \sqrt{S_{12}^2 + S_{22}^2 + S_{32}^2 + S_{42}^2 + S_{52}^2 + S_{62}^2 + S_{72}^2}$$

$$S_2 = [\,34.481^2 + 34.481^2 + 34.481^2 + 34.481^2 + 48.270^2 + 68.953^2 + 48.270^2\,]^{1/2}$$

$$= 119.039 \text{ P}_a \tag{46}$$

$$\nu_2 = \frac{(S_{12}^2 + S_{22}^2 + S_{32}^2 + S_{42}^2 + S_{52}^2 + S_{62}^2 + S_{72}^2)^2}{\left(\frac{S_{12}^4}{\nu_{12}} + \frac{S_{22}^4}{\nu_{22}} + \frac{S_{32}^4}{\nu_{32}} + \frac{S_{42}^4}{\nu_{42}} + \frac{S_{52}^4}{\nu_{52}} + \frac{S_{62}^4}{\nu_{62}} + \frac{S_{72}^4}{\nu_{72}}\right)}$$

$$\nu_2 = (34.481^2 + 34.481^2 + 34.481^2 + 34.481^2 + 48.270^2 + 68.953^2 + 48.270^2)^2 \Big/ \left(\frac{34.481^4}{40} + \frac{34.481^4}{90} + \frac{34.481^4}{200} + \frac{34.481^4}{10} + \frac{48.270^4}{100} + \frac{68.953^4}{10} + \frac{48.270^4}{60}\right) = 77 \tag{47}$$

0260r

The systematic error limit for the data acquisition process is x

$$B_2 = [\,68.953^2 + 68.953^2 + 68.953^2 + 68.953^2$$
$$+ 68.953^2 + 68.953^2 + 117.223^2\,]^{1/2}$$
$$= 205.6\ P_a \quad (48)$$

A computer operates on raw pressure measurement data to perform the conversion to engineering units. Errors in this process are called data reduction errors and stem from curve fits and computer resolution.

Computer resolution is the source of a small elemental error. Some of the smallest computers used in experimental test applications have six digits resolution. The resolution error is then plus or minus one in 10^6. Even though this error is probably negligible, consideration should be given to rounding off and truncating errors. Rounding-off results in a random error. Truncating always results in a systematic error (assumed in this example.)

Table 9 lists data reduction error sources.

Table 9 — Pressure measurement data reduction error sources

Error source	*Systematic error, P_a*	*Experimental standard deviation, P_a*	*Degrees of freedom*
Curve Fit	B_{13} = 68.953	S_{13} = 0	v_{13}
Computer Resolution	B_{23} = 6.894	S_{23} = 0	v_{23}

The experimental standard deviation for the data reduction process is

$$S_3 = \sqrt{S_{13}^2 + S_{23}^2}$$
$$= 0.0 \quad (49)$$

The systematic error limit for the data reduction process is

$$B_3 = \sqrt{B_{13}^2 + B_{23}^2}$$
$$B_3 = \sqrt{68.953^2 + 6.894^2}$$
$$= 69.297\ P_a \quad (50)$$

The experimental sample standard deviation for pressure measurement then is

$$S_p = [\,S_{11}^2 + S_{21}^2 + S_{31}^2 + S_{41}^2 + S_{12}^2 + S_{22}^2 + S_{32}^2$$
$$+ S_{42}^2 + S_{52}^2 + S_{62}^2 + S_{72}^2 + S_{13}^2 + S_{23}^2\,]^{1/2} \quad (51)$$

or

$$S_p = \sqrt{S_1^2 + S_2^2 + S_3^2}$$
$$= \sqrt{43.651\,9^2 + 119.039^2 + 0.0^2}$$
$$= 126.790\ P_a \quad (52)$$

Degrees of freedom associated with the experimental standard deviation are determined as follows:

$$v_p = (S_{11}^2 + S_{21}^2 + S_{31}^2 + S_{41}^2 + S_{12}^2 + S_{22}^2 + S_{32}^2 + S_{42}^2 + S_{52}^2 + S_{62}^2$$
$$+ S_{72}^2 + S_{13}^2 + S_{23}^2)^2$$
$$\Big/ \left(\frac{S_{11}^4}{v_{11}} + \frac{S_{21}^4}{v_{21}} + \frac{S_{31}^4}{v_{31}} + \frac{S_{41}^4}{v_{41}} + \frac{S_{12}^4}{v_{12}} + \frac{S_{22}^4}{v_{22}} + \frac{S_{32}^4}{v_{32}} + \frac{S_{42}^4}{v_{42}} \right.$$
$$\left. + \frac{S_{52}^4}{v_{52}} + \frac{S_{62}^4}{v_{62}} + \frac{S_{72}^4}{v_{72}} + \frac{S_{13}^4}{v_{13}} + \frac{S_{23}^4}{v_{23}} \right) \quad (53)$$

or

$$\nu_p = \frac{(S_1^2 + S_2^2 + S_3^2)^2}{\left(\frac{S_1^4}{\nu_1} + \frac{S_2^4}{\nu_2} + \frac{S_3^4}{\nu_3} \right)}$$

$$\nu_p = \frac{(43.651\,9^2 + 119.039^2 + 0.0^2)^2}{\left(\frac{43.651\,9^4}{54} + \frac{119.039^4}{77} + \frac{0.0^4}{0} \right)}$$

$$= 96 \text{ therefore } t_{95} = 2. \qquad (54)$$

The systematic error limit for the pressure measurement is

$$B_p = [\, B_{11}^2 + B_{21}^2 + B_{31}^2 + B_{41}^2 + B_{12}^2 + B_{22}^2 + B_{32}^2 + B_{42}^2 + B_{52}^2 + B_{62}^2 + B_{72}^2 + B_{13}^2 + B_{23}^2]^{1/2} \qquad (55)$$

or

$$B_p = \sqrt{B_1^2 + B_2^2 + B_3^2}$$

$$B_p = \sqrt{172.246^2 + 205.593^2 + 69.297^2}$$

$$= 277.018 \text{ P}_a \qquad (56)$$

Uncertainty for the pressure measurement is

$$U_{99} = (B_p + t_{95} S_p),\ U_{95} = \sqrt{B_p^2 + (t_{95} S_p)^2}$$

$$U_{99} = (277.018 + 2 \times 126.790)$$

$$= 530.598 \text{ P}_a,\ U_{95} = 375.6 \text{ P}_a \qquad (57)$$

A.2.2.2 The calibration hierarchy for temperature measurements is similar to that for pressure measurements. Figure 16 depicts a typical temperature measurement hierarchy. As in the pressure calibration hierarchy, each comparison in the temperature calibration hierarchy may produce elemental systematic and random errors. Table 10 lists temperature calibration hierarchy elemental errors.

Table 10 — Temperature calibration hierarchy elemental errors

Calibration	*Systematic error, K*	*Experimental standard deviation, K*	*Degrees of freedom*
SL - ILS	$B_{11} = 0.056$	$S_{11} = 0.002$	$\nu_{11} = 2$
ILS-TS	$B_{21} = 0.278$	$S_{21} = 0.028$	$\nu_{21} = 10$
TS - WS	$B_{31} = 0.333$	$S_{31} = 0.028$	$\nu_{31} = 15$
WS - MI	$B_{41} = 0.378$	$S_{41} = 0.039$	$\nu_{41} = 30$

The calibration hierarchy experimental standard deviation is calculated as

$$S_1 = \sqrt{S_{12}^2 + S_{21}^2 + S_{31}^2 + S_{41}^2}$$

$$= \sqrt{0.002^2 + 0.028^2 + 0.028^2 + 0.039^2}$$

$$= 0.056\ ^\circ\text{K}. \qquad (58)$$

Degrees of freedom associated with S_1 are

$$\nu_1 = \frac{(S_{11}^2 + S_{21}^2 + S_{31}^2 + S_{41}^2)^2}{\left(\frac{S_{11}^4}{\nu_{11}} + \frac{S_{21}^4}{\nu_{21}} + \frac{S_{31}^4}{\nu_{31}} + \frac{S_{41}^4}{\nu_{41}} \right)}$$

$$= \frac{(0.002^2 + 0.028^2 + 0.028^2 + 0.039^2)^2}{\left(\frac{0.002^4}{2} + \frac{0.028^4}{10} + \frac{0.028^4}{15} + \frac{0.039^4}{30} \right)}$$

$$= 53 > 30, \text{ therefore } t_{95} = 2. \qquad (59)$$

The calibration hierarchy systematic error limit is

$$B_1 = \sqrt{B_{11}^2 + B_{21}^2 + B_{31}^2 + B_{41}^2} \qquad (60)$$

$$= \sqrt{0.056^2 + 0.278^2 + 0.333^2 + 0.378^2} \qquad (61)$$

$$= 0.578\ ^\circ\text{K}.$$

A reference temperature monitoring system will provide an excellent source of data for evaluating both data acquisition and reduction temperature random errors.

Figure 17 depicts a typical setup for measuring temperature with Chromel-Alumel thermocouples.

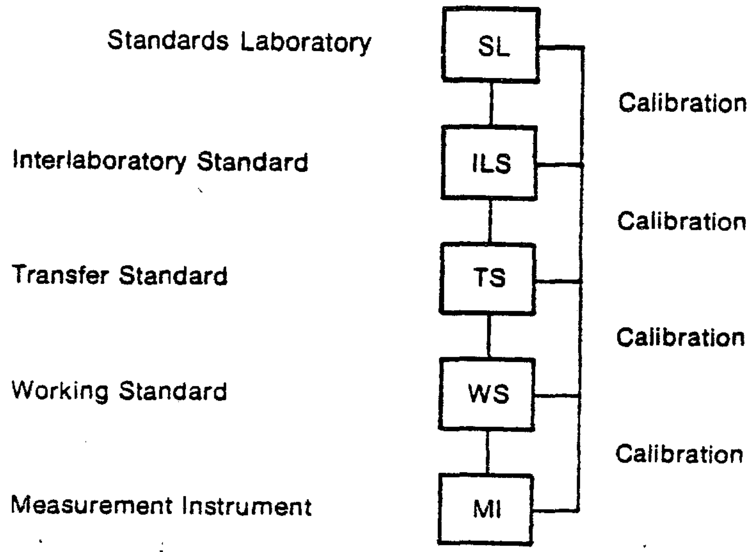

Figure 16 — Temperature measurement calibration hierarchy

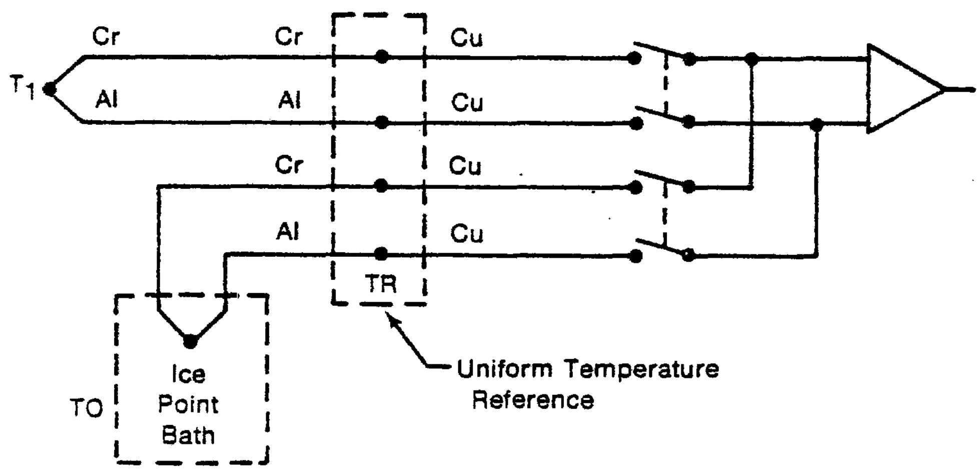

Figure 17 — Typical thermocouple channel

If several calibrated thermocouples are utilized to monitor the temperature of an ice point bath, statistically useful data can be recorded each time measurement data are recorded. Assuming that those thermocouple data are recorded and reduced to engineering units by processes identical to those employed for test temperature measurements, a stockpile of data will be gathered, from which data acquisition and reduction errors may be estimated.

For the purpose of illustration, suppose N calibrated Chromel-Alumel thermocouples are employed to monitor the ice bath temperature of a temperature measuring system similar to that depicted by figure 17. If each time measurement data are recorded, multiple scan recordings are made for each of the thermocouples, and if a multiple scan average (X_{ij}) is calculated for each thermocouple, then the average ($\overline{X}_j$) for all recordings of the jth thermocouple is

$$\overline{X}_j = \frac{\sum_{i=1}^{k_j} X_{ij}}{K_j} \tag{62}$$

where K_j is the number of multiple scan recordings for the jth thermocouple.

The grand average ($\overline{X}$) is computed for all monitor thermocouples as

$$\overline{X} = \frac{\sum_{j=1}^{N} \overline{X}_j}{N} . \tag{63}$$

The experimental standard deviation ($S_{\overline{x}}$) for the data acquisition and reduction processes is then

$$S_{\overline{x}} = \sqrt{\frac{\sum_{j=1}^{N}\sum_{i=1}^{K_j} (X_{ij} - \overline{X}_j)^2}{\sum_{j=1}^{N} (K_j - 1)}} \tag{64}$$

$$= 0.094 \text{ K (assumed for this example)}$$

The degrees of freedom associated with $S_{\overline{x}}$ are

$$\nu_{\overline{x}} = \sum_{j=1}^{N} (K_j - 1) \tag{65}$$

$$= 200 \text{ (assumed for this example)}$$

Data acquisition and reduction systematic error limits may be evaluated from the same ice bath temperature data if the temperature of the ice bath is continuously measured with a working standard such as a calibrated mercury-in-glass thermometer. There the systematic error limit is the largest observed difference between $\overline{X}$ and the temperature indicated by the working standard acquisition and reduction process. In this example, it is assumed to be 0.56°K, i.e.,

$$B_{\overline{x}} = 0.56\text{°K} \tag{66}$$

Error sources accounted for by this method are:

1) Ice point bath reference random error
2) Reference block temperature random error
3) Recording system resolution error
4) Recording system electrical noise error
5) Analog-to-digital conversion error
6) Chromel-Alumel thermocouple millivolt output vs. temperature curve-fit error
7) Computer resolution error

Several errors which are not included in the monitoring system statistics are:

1) Conduction error (B_C)
2) Radiation error (B_R)
3) Recovery error (B_Y)
4) Calibration error (B_1)

These errors are a function of probe design and environmental conditions. Detailed treatment of these error sources is beyond the scope of this work.

The experimental standard deviation for temperature measurements in this example is

$$S_\tau = \sqrt{S_1^2 + S_{\overline{x}}^2} \tag{67}$$

where

S_1 = calibration hierarchy experimental standard deviation

0260r

$S_{\bar{x}}$ = data acquisition and reduction experimental standard deviation

$$S_\tau = \sqrt{0.056^2 + 0.094^2}$$

$$= 0.11\ ^\circ K$$

The degrees of freedom associated with S_τ are

$$\nu_\tau = \frac{(S_1^2 + S_2^2)^2}{\left(\frac{S_1^4}{\nu_1} + \frac{S_2^4}{\nu_2}\right)} \tag{68}$$

$$\nu_\tau = \frac{(0.056^2 + 0.094^2)^2}{\left(\frac{0.056^4}{53} + \frac{0.094^4}{200}\right)}$$

$$= 250 \text{ therefore } t_{95} = 2$$

Systematic error limits for the measurements are

$$B_\tau = \sqrt{B_1^2 + B_{\bar{x}}^2 + B_C^2 + B_R^2 + B_Y^2} \tag{69}$$

where

B_1 = calibration hierarchy systematic error limits

$B_{\bar{x}}$ = data acquisition and reduction systematic error limits

B_C = conduction error systematic error limits (negligible in this example)

B_R = radiation error systematic error limits (negligible in this example)

B_Y = recovery factor systematic error limits (negligible in this example)

$$B_\tau = \sqrt{0.578^2 + 0.56^2}$$

$$= 0.804^\circ K$$

Uncertainty for the temperature measurement is

$$U_\tau = (B_\tau + t_{95}\, S_\tau)$$

$$U_{99} = (B_\tau + t_{95}\, S_\tau),\ U_{95} = \sqrt{B_\tau^2 + (t_{95}\, S_\tau)^2}$$

$$U_{99} = (0.804 + 2 \times 0.11),\ U_{95} = \sqrt{0.804^2 + (2 \times 0.11)^2}$$

$$= 1.02^\circ K, \qquad = 0.83^\circ K \tag{70}$$

When ν is less than 30, t_{95} is determined from a Student's t table at the value of ν. Since ν_τ is greater than 30 here, use $t_{95} = 2$.

A.2.2.3 There are catalogs of discharge coefficients for a variety of venturis, nozzles and orifices. Cataloged values are the result of a large number of actual calibrations over a period of many years. Detailed engineering comparisons must be exercised to ensure that the flowmeter conforms to one of the groups tested before using the tabulated values for discharge coefficients and error tolerances.

To minimize the uncertainty in the discharge coefficient, it should be calibrated using primary standards in a recognized laboratory. Such a calibration will determine a value of A_{eff} = Ca and the associated systematic error limit and experimental standard deviation.

When an independent flowmeter is used to determine flowrates during a calibration for C, dimensional errors are effectively calibrated out. However, when C is calculated or taken from a standard reference, errors in the measurement of pipe and throat diameters will be reflected as systematic errors in the flow measurement.

Dimensional errors in large venturis, nozzles and orifices may be negligible. For example, an error of 0.001 inch in the throat diameter of a 5 inch critical flow nozzle will result in a 0.04% systematic error in airflow. However, these errors can be significant at large diameter ratios.

A.2.2.4 Non-ideal gas behavior and changes in gas composition are accounted for by selection of the proper values for compressibility factor (Z), molecular weight (M) and ratio of specific heats (γ) for the specific gas flow being measured.

When values of γ and Z are evaluated at the proper pressure and temperature conditions, airflow errors resulting from errors in γ and Z will be negligible.

For the specific case of airflow measurement, the main factor contributing to variation of composition is the moisture content of the air. Though small, the effect of a change in air density due to water vapor on airflow measurement should be evaluated in every measurement process.

A.2.2.5 The thermal expansion correction factor (F_a) corrects for changes in throat area caused by changes in flowmeter temperature.

For steels, a 17°K flowmeter temperature difference, between the time of a test and the time of calibration, will introduce an airflow error of 0.06% if no correction is made. If flowmeter skin temperature is determined to within 3°K and the correction factor applied, the resulting error in airflow will be negligible.

A.2.3 Propagation of error to airflow

For an example of propagation of errors in airflow measurement using a critical-flow venturi, consider a venturi having a throat diameter of 0.554 meters operating with dry air at an upstream total pressure of 88 126P_a and an upstream total temperature of 265.9°K.

Equation (71) is the flow equation to be analyzed:

$$W = \frac{\pi d^2}{4} C F_a \varphi^* \frac{P_1}{\sqrt{T_1}}$$

$$\varphi^* = \sqrt{\left(\frac{2}{\gamma + 1}\right)^{\frac{\gamma+1}{\gamma-1}} \left(\frac{\gamma g M}{ZR}\right)} \qquad (71)$$

Assume, for this example, that the theoretical discharge coefficient (C) has been determined to be 0.995. Further assume that the thermal expansion correction factor (F_a) and the compressibility factor (Z) are equal to 1.0. Table 11 lists nominal values, systematic error limits, sample standard deviations and degrees of freedom for each error source in the above equation. (To illustrate the uncertainty methodology, we will assume a sample standard deviation of 0.000 5 in addition to a systematic error of 0.003.)

Note that, in table 11, airflow errors resulting from errors in F_a, Z, k, g, M and R are considered negligible.

Table 11 — Airflow measurement error sources

Error source	*Units*	*Nominal value*	*Systematic error limit*	*Experimental standard deviation*	*Degrees of freedom, ν*	*Uncertainty U_{99}*
P_1	P_a	88 126	277.02	126.79	96	530.60
T_1	K	265.9	0.8	0.11	250	1.02
d	m	0.554	2.54×10^{-5}	2.54×10^{-5}	100	7.62×10^{-5}
C		0.995	0.003	0.000 5	—	0.003
F_a		1.0	—	—	—	—
Z		1.0	—	—	—	—
γ		1.401	—	—	—	—
g		—	—	—	—	—
M	kg/kg-mole	28.95	—	—	—	—
R	J/K-kg-mole	8.314	—	—	—	—

From equation (71), airflow is calculated as

$$W = \frac{3.142}{4}(0.554)^2 \times 0.995 \times 1.0 \times \sqrt{\left(\frac{2}{2.401}\right)^{\frac{2.401}{0.401}} \left(\frac{1.401 \times 28.95}{8\,314}\right) \times \frac{88\,126}{\sqrt{265.9}}}$$

$$= 52.39 \text{ kg/sec.}$$

Taylor's series expansion of equation (71) with the assumptions indicated yields equations (72) and (73) from which the flow measurement experimental standard deviation and systematic error limits are calculated.

$$S_w = W\sqrt{\left(\frac{S_{P_1}}{P_1}\right)^2 + \left(\frac{-S_{T_1}}{2T_1}\right)^2 + \left(\frac{S_C}{C}\right)^2 + \left(\frac{2S_d}{d}\right)^2}$$

$$S_w = 52.39\left[\left(\frac{126.790}{88\,126}\right)^2 + \left(\frac{-0.11}{2 \times 265.9}\right)^2 + \left(\frac{0.000\,5}{995}\right)^2 + \left(\frac{2 \times 0.000\,025}{0.554}\right)^2\right]^{1/2}$$

$$= 52.39\sqrt{(0.001\,4)^2 + (-0.000\,2)^2 + (0.000\,503)^2 + (0.000\,09)^2}$$

$$= 0.078\,7 \text{ kg/sec} \quad (72)$$

$$B_w = W\sqrt{\left(\frac{B_{P_1}}{P_1}\right)^2 + \left(\frac{-B_{T_1}}{2T_1}\right)^2 + \left(\frac{B_C}{C}\right)^2 + \left(\frac{2B_d}{d}\right)^2}$$

$$B_w = 52.39\left[\left(\frac{277.02}{88\,126}\right)^2 + \left(\frac{-0.804}{531.8}\right)^2 + \left(\frac{0.003}{0.995}\right)^2 + \left(\frac{0.000\,05}{0.554}\right)^2\right]^{1/2}$$

$$= 52.39\sqrt{(0.003\,1)^2 + (-0.001\,5)^2 + (0.003\,0)^2 + (0.000\,09)^2}$$

$$= 0.241\,6 \text{ kg/seg} \quad (73)$$

By using the Welch-Satterthwaite formula, the degrees of freedom for the combined experimental standard deviation is determined from

$$\nu_w = \frac{\left[\left(\frac{\partial W}{\partial P_1}S_{P_1}\right)^2 + \left(\frac{\partial W}{\partial T_1}S_{T_1}\right)^2 + \left(\frac{\partial W}{\partial d}S_d\right)^2 + \left(\frac{\partial W}{\partial C}S_C\right)^2\right]^2}{\frac{\left(\frac{\partial W}{\partial P_1}S_{P_1}\right)^4}{\nu_{P_1}} + \frac{\left(\frac{\partial W}{\partial T_1}S_{T_1}\right)^4}{\nu_{T_1}} + \frac{\left(\frac{\partial W}{\partial d}S_4\right)^4}{\nu_d} + \frac{\left(\frac{\partial W}{\partial C}S_C\right)^4}{\nu_C}}$$

$$= \frac{\left[\left(\frac{S_{P_1}}{P_1}\right)^2 + \left(\frac{-S_{T_1}}{2T_1}\right)^2 + \left(\frac{2S_d}{d}\right)^2 + \left(\frac{S_C}{C}\right)^2\right]^2}{\frac{\left(\frac{S_{P_1}}{P_1}\right)^4}{\nu_{P_1}} + \frac{\left(\frac{-S_{T_1}}{2T_1}\right)^4}{\nu_{T_1}} + \frac{\left(\frac{2S_d}{d}\right)^4}{\nu_d} + \frac{\left(\frac{S_C}{C}\right)^4}{\nu_C}} \quad (74)$$

which results in an overall degrees of freedom > 30, and, therefore, a value of t_{95} of 2.0.

Total airflow uncertainty is then,

$$U_{99} = (B_w + t_{95}\,S_w),\ U_{95} = \sqrt{B_w^2 + (t_{95}\,S_w)^2}$$

$$U_{99} = [0.241\,6 + 2 \times 0.078\,7]$$

$$= 0.40 \text{ kg/sec}$$

$$= 0.8\%$$

$$U_{95} = 0.29 \text{ kg/sec}$$

$$= 0.55\% \quad (75)$$

A.3 Example two — comparative test

A.3.1 Definition of the measurement process

The objective of a comparative test is to determine with the smallest measurement uncertainty the net effect of a design change, such as a new part. The first test is performed with the standard or baseline configuration. A second test, identical to the first except that the design change is substituted in the baseline configuration, is then carried out. The difference between the measurement results of the two tests is an indication of the effect of the design change.

As long as we only consider the difference or net effect between the two tests, all the fixed, constant, systematic errors will cancel out. The measurement uncertainty is composed of random errors only.

For example, assume we are testing the effect on the gasflow of a centrifugal compressor from a change to the inlet inducer. At constant inlet and discharge conditions, and constant rotational speed, will the gas flow increase? If we test the compressor with the old and new inducers and take the difference in measured airflow as our defined measurement process, we obtain the smallest uncertainty. All the systematic errors cancel. Note that, although the comparative test provides an accurate net effect, the absolute value (gasflow with the new inducer) is not determined or if calculated, as in example one, it will be inflated by the systematic errors. Also, the small uncertainty of the comparative test can be significantly reduced by repeating it several times.

A.3.2 Measurement error sources

All errors result from random errors in data acquisition and data reduction. Systematic errors are effectively zero. Random error values are identical to those in example one, except that calibration random errors become systematic errors and, hence, effectively zero.

A.3.2.1 Comparative tests shall use the same test facility and instrumentation for each test. All calibration errors are systematic and cancel out in taking the difference between the test results.

$$B_1 = 0$$

and

$$S_1 = 0, S_C = 0$$

A.3.2.2

$$S_p = S_2$$

$$= 119.039 \text{ Pa}$$

(see equation (47))

$$\nu_p = \nu_2 = 77$$

(see equation (48))

$$S_\tau = S_{\bar{x}}$$

$$= 0.094^\circ\text{K}$$

(see equation (64))

$$\nu_\tau = \nu_{\bar{x}}$$

$$= 200$$

(see equation (65))

A.3.2.3 The test result is the difference in flow between two tests.

$$\Delta_w = W_1 - W_2$$

$$S_{\Delta w} = \sqrt{S_{w1}^2 + (-1)^2 S_{w2}^2} = S_w \sqrt{2}$$

$$U_{\Delta w_{99}} = (B_{\Delta w} + 2S_{\Delta w}) \qquad U_{\Delta w_{95}} = \sqrt{(B_{\Delta w})^2 + (2S_{\Delta w})^2}$$

$$= (0 + 2S_{\Delta w}) \qquad = \sqrt{0^2 + (2S_{\Delta w})^2}$$

$$= 2S_{\Delta w} \qquad = 2S_{\Delta w}$$

$$U_{\Delta w_{99}} = 2S_w \sqrt{2} \qquad U_{\Delta w_{95}} = 2S_w \sqrt{2}$$

$$S = \pm 52.39 \left[\left(\frac{119.037}{88\,126} \right)^2 + \left(\frac{-0.094}{2 \times 265.9} \right)^2 + \left(\frac{0.000\,5}{0.995} \right)^2 + \left(\frac{0.000\,05}{0.554} \right)^2 \right]^{1/2}$$

$$S_w = 0.076\,2 \text{ kg/sec} \qquad S_{\Delta w} = 0.107\,8 \text{ kg/sec}$$

$$U_{\Delta w_{99}} = 0.215\,5 \text{ kg/sec} \qquad U_{\Delta w_{95}} = 0.215\,5 \text{ kg/sec}$$

$$= 0.41\% \qquad = 0.41\%$$

(see equation (75))

A.3.2.4 Note that the differences shown in table 12 are entirely due to differences in the measurement process definitions. The same fluid flow measurement system might be used in both examples. The comparative test has the smallest measurement uncertainty, but this uncertainty value does not apply to the measurement of absolute level of fluid flow, only to the difference.

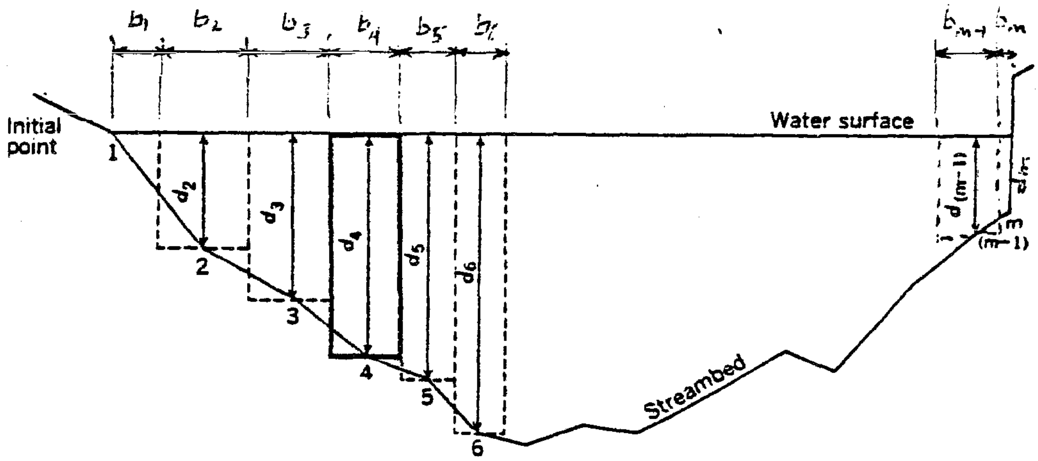

Explanation

1, 2, 3, ... m	Observation points
$b_1, b_2, b_3, .. b_m$	Breadth (metres) of segment associated with the observation point
$d_1, d_2, d_3, .. d_m$	Depth of water (metres) at the observation point
Dashed lines	Boundary of segments: one heavily outlined

If x and y are respectively horizontal and vertical coordinates of all the points in the cross-section, and A is its total area, then the precise mathematical expression for q_v, the true volumetric flowrate (discharge) across the area, can be written as

Figure 18 — Definition sketch of velocity-area method of discharge measurement (midsection method)